ICA Color Space for Pattern Recognition

Chengjun Liu and Jian Yang

Abstract—This paper presents a novel independent component analysis (ICA) color space method for pattern recognition. The novelty of the ICA color space method is twofold: 1) deriving effective color image representation based on ICA, and 2) implementing efficient color image classification using the independent color image representation and an enhanced Fisher model (EFM). First, the ICA color space method assumes that each color image is defined by three independent source images, which can be derived by means of a blind source separation procedure, such as ICA. Unlike the RGB color space, where the R, G, and B component images are correlated, the new ICA color space method derives three component images C_1, C_2, and C_3 that are independent and hence uncorrelated. Second, the three independent color component images are concatenated to form an augmented pattern vector, whose dimensionality is reduced by principal component analysis (PCA). An EFM then derives the discriminating features of the reduced pattern vector for pattern recognition. The effectiveness of the proposed ICA color space method is demonstrated using a complex grand challenge pattern recognition problem and a large scale database. In particular, the face recognition grand challenge (FRGC) and the biometric experimentation environment (BEE) reveal that for the most challenging FRGC version 2 Experiment 4, which contains 12 776 training images, 16 028 controlled target images, and 8014 uncontrolled query images, the ICA color space method achieves the face verification rate (ROC III) of 73.69% at the false accept rate (FAR) of 0.1%, compared to the face verification rate (FVR) of 67.13% of the RGB color space (using the same EFM) and 11.86% of the FRGC baseline algorithm at the same FAR.

Index Terms—Biometric experimentation environment (BEE), enhanced Fisher model (EFM), face recognition grand challenge (FRGC), independent component analysis (ICA) color space, pattern recognition, principal component analysis (PCA), RGB color space.

I. INTRODUCTION

A color image, determined by a function of two spatial variables and one spectral variable, is 3-D and multispectral [14]. The spectral dimension is usually sampled to the red (R), green (G), and blue (B) spectral bends, known as the primary colors. A color image, therefore, contains three component images: the red, green, and blue component images. Each pixel of a color image is specified in a color space, which serves as a color coordinate system. One commonly used color space is the RGB color space, and other color spaces are usually calculated from the RGB color space by means of either linear or nonlinear transformations.

As different color spaces transformed from the RGB color space display different discriminating power for pattern recognition [10], [23], [34], this paper seeks a novel independent component analysis (ICA) color space method for both effective color image representation and efficient color image classification. First, the ICA color space method assumes that each color image is defined by three independent source images, C_1, C_2, and C_3, which can be derived by means of a blind source separation procedure, such as ICA [7], [22]. Second, the three independent color component images are concatenated to form an augmented pattern vector, whose dimensionality is reduced by principal component analysis (PCA) [11]. Specifically, the three images C_1, C_2, and C_3 are first converted into vectors, respectively. Each of the three vectors is then normalized to zero mean and unit variance. The three normalized vectors are finally concatenated to form the augmented pattern vector. An enhanced Fisher model (EFM) [25] then derives the discriminating features of the reduced pattern vector for pattern recognition.

The novelty of the ICA color space method is twofold: 1) deriving effective color image representation based on ICA, and 2) implementing efficient color image classification using the independent color image representation and an EFM. The motivation of investigating an ICA color space rests on the findings that ICA provides a powerful data representation method for pattern recognition [1], [7], [22]. ICA derives a linear transformation to represent a set of random variables as linear combinations of statistically independent source variables [7]. The search criterion involves the minimization of the mutual information defined as a function of high-order statistics (cumulants). While PCA applies low-order (≤ 2) statistics (mean, variance, and covariance) to uncorrelate data, ICA would further reduce statistical dependencies and produce a sparse and independent code useful for subsequent pattern discrimination [30]. Unlike the RGB color space, where the R, G, and B component images are correlated, the new ICA color space method derives three component images C_1, C_2, and C_3 that are independent and hence uncorrelated.

The effectiveness of the proposed ICA color space method is demonstrated using a complex grand challenge pattern recognition problem and a large scale database. In particular, the face recognition grand challenge (FRGC) [32] and the biometric experimentation environment (BEE) [32] reveal that for the most challenging FRGC version 2 Experiment 4, which contains 12 776 training images, 16 028 controlled target

C. Liu is with the Department of Computer Science, New Jersey Institute of Technology, Newark, NJ 07102 USA (e-mail: chengjun.liu@njit.edu).

J. Yang was with the Department of Computer Science, New Jersey Institute of Technology, Newark, NJ 07102 USA. He is now with the School of Computer Science and Technology, Nanjing University of Science and Technology, Nanjing 210094, China (e-mail: csjyang@njit.edu).

images, and 8014 uncontrolled query images, the ICA color space method achieves the face verification rate (ROC III) of 73.69% at the false accept rate (FAR) of 0.1%, compared to the face verification rate (FVR) of 67.13% of the RGB color space (using the same EFM) and 11.86% of the FRGC baseline algorithm at the same FAR.

II. BACKGROUND

Color has been widely applied in machine learning and pattern recognition [10], [13]. Color invariant moments and color histograms, for example, are efficient cue for indexing into a large image database or for object recognition against image variations such as illumination [9], [15], [35], [37]. Different color spaces defined by transformations from the RGB color space possess different color characteristics, which can be applied for different visual tasks, such as object detection, indexing and retrieval, and recognition [10], [13], [18], [27], [28], [39]. For instance, the HSV (hue, saturation, value) color space and the $YCbCr$ (luminance, chrominance-blue, chrominance-red) color space have been applied for face detection by many researchers [12], [17], [18], [36], [40]. Different color spaces also reveal different discriminating power for pattern recognition [10], [23], [34]. The R component image in the RGB color space and the V component image in the HSV color space, for example, have been shown more effective for face recognition than the component images in several other color spaces [34]. Jones and Abbott [21] propose a conversion of color images to a monochromatic form, namely, from a 3-D color space to a 1-D space, for improving human face recognition performance upon the grayscale images. Neagoe [29] presents a color conversion using Karhunen–Loeve transform (KLT) or PCA, namely, from the 3-D RGB color space to a 2-D PCA color space, for pattern recognition using a concurrent neural network classifier, and demonstrates the feasibility of the method on face recognition.

Face recognition has become a very active research area in pattern recognition driven mainly by its broad applications in human–computer interaction, homeland security, and entertainment [4]–[6], [20], [31], [42]. To promote and advance face recognition technologies, the National Institute of Standards and Technology (NIST), sponsored by multiple U.S. government agencies, conducted the face recognition grand challenge program or FRGC [32]. FRGC consists of a number of experiments, and the FRGC baseline algorithm reveals that the FRGC version 2 Experiment 4, which is designed for controlled single still image versus uncontrolled single still image, is the most challenging FRGC experiment. The grand challenges are caused mainly by those uncontrolled factors such as the large illumination variations. The data contained in the FRGC version 2 Experiment 4 includes 12 776 training images, 16 028 controlled target images, and 8014 uncontrolled query images. Face recognition performance is reported using the receiver operating characteristic (ROC) curves, which plot the FVR versus the FAR. The biometric experimentation environment system or BEE generates three ROC curves (ROC I, ROC II, and ROC III) corresponding to the images collected within semesters, within a year, and between semesters, respectively [32]. Note that the FRGC baseline algorithm, which is a PCA
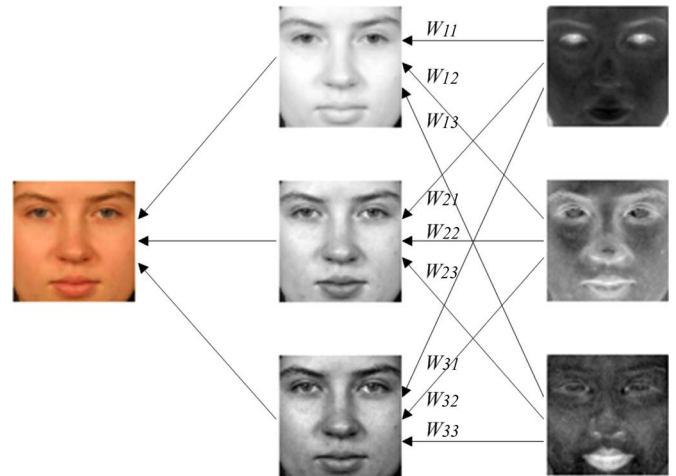

Fig. 1. Architecture of the ICA color space method. An image in the first column consists of three color component images $\mathbf{R}$, $\mathbf{G}$, and $\mathbf{B}$ shown in the middle column. The three images in the right column are the independent source images $\mathbf{C}_1$, $\mathbf{C}_2$, and $\mathbf{C}_3$, derived using ICA. The three correlated $\mathbf{R}$, $\mathbf{G}$, and $\mathbf{B}$ component images are defined by the linear combinations of the three independent source images $\mathbf{C}_1$, $\mathbf{C}_2$, and $\mathbf{C}_3$ with weights W_{ij} $(i, j = 1, 2, 3)$.

algorithm optimized for large scale problems [3], [26], [32], achieves the FVR (ROC III) of 11.86% at the FAR 0.1%, using the grayscale image that is the average of the three R, G, and B component images.

III. ICA COLOR SPACE FOR EFFECTIVE COLOR IMAGE REPRESENTATION

In the RGB color space, a color image $\mathbf{C}$ with a spatial resolution of $m \times n$ contains three color component images $\mathbf{R}$, $\mathbf{G}$, and $\mathbf{B}$ with the same resolution of $m \times n$. Each pixel of the color image $\mathbf{C}$ thus resides in a 3-D space: $\mathcal{X} \in \mathbb{R}^3$, where the elements of $\mathcal{X}$ are the red, green, and blue values from the $\mathbf{R}$, $\mathbf{G}$, and $\mathbf{B}$ component images, respectively. As the $\mathbf{R}$, $\mathbf{G}$, and $\mathbf{B}$ component images are correlated, the elements of the random vector $\mathcal{X}$ are also correlated. Recent research reveals that different color spaces transformed from the RGB color space display different discriminating power for pattern recognition [10], [23], [34]. This paper, therefore, investigates a novel ICA color space method for effective color image representation, which can help improve pattern recognition performance.

The ICA color space method assumes that every color image is defined by three independent source images $\mathbf{C}_1$, $\mathbf{C}_2$, and $\mathbf{C}_3$, which can be derived by means of a blind source separation procedure, such as ICA [7], [22]. Fig. 1 shows the architecture of the ICA color space method. Specifically, a color image $\mathbf{C}$ in the RGB color space contains three color component images $\mathbf{R}$, $\mathbf{G}$, and $\mathbf{B}$ shown in the middle column. These correlated $\mathbf{R}$, $\mathbf{G}$, and $\mathbf{B}$ component images are defined by means of the linear combinations (with weights W_{ij}, where $i, j = 1, 2, 3$) of the three independent source images $\mathbf{C}_1$, $\mathbf{C}_2$, and $\mathbf{C}_3$ (in the last column) derived using ICA. As ICA provides a powerful data representation method for pattern recognition [1], [7], [22], the ICA color space is expected to possess more discriminating power than the RGB color space.

ICA of a random vector seeks a linear transformation that minimizes the statistical dependence among the elements of the

vector [7], [16], [33], [41]. We apply independent component analysis to the 3-D pattern vector $\mathcal{X}$, whose elements correspond to the red, green, and blue values from the $\mathbf{R}$, $\mathbf{G}$, and $\mathbf{B}$ component images of the color image $\mathbf{C}$. In particular, the covariance matrix of $\mathcal{X}$ is defined as: $\Sigma_{\mathcal{X}} = \mathcal{E}\{[\mathcal{X} - \mathcal{E}(\mathcal{X})][\mathcal{X} - \mathcal{E}(\mathcal{X})]^t\}$, where $\mathcal{E}(\cdot)$ is the expectation operator, t denotes the transpose operation, and $\Sigma_{\mathcal{X}} \in \mathbb{R}^{3 \times 3}$ is a real and symmetric square matrix. Note that $\Sigma_{\mathcal{X}}$ can be estimated using the sample covariance matrix of the 3-D pattern vectors of all the training color images (with mn 3-D pattern vectors in each training color image). The ICA of the 3-D pattern vector $\mathcal{X}$ factorizes the covariance matrix $\Sigma_{\mathcal{X}}$ into the following form:

$$\Sigma_{\mathcal{X}} = W \nabla W^t \tag{1}$$

where $\nabla \in \mathbb{R}^{3 \times 3}$ is diagonal real positive and $W \in \mathbb{R}^{3 \times 3}$, defined by the weights (W_{ij}, where $i, j = 1, 2, 3$) of the linear combinations in the architecture of the ICA color space method (see Fig. 1), transforms the original pattern vector $\mathcal{X} \in \mathbb{R}^3$ to a new 3-D pattern vector $\mathcal{Z} \in \mathbb{R}^3$

$$\mathcal{X} = W\mathcal{Z}. \tag{2}$$

The three components of the new pattern vector $\mathcal{Z}$ are independent or the most independent possible. Note that (1) is not just a PCA decomposition, because PCA can only derive uncorrelated principal components rather than independent components. To derive the W matrix in (2), Comon [7] develops an algorithm by calculating mutual information and high-order statistics. Next, we briefly review some high points of Comon's ICA algorithm in order to explain the three major steps applied to derive the independent pattern vector $\mathcal{Z}$ in (2).

Let the probability density function of the random vector $\mathcal{Z} \in \mathbb{R}^k$ be $p_z(\mathbf{z})$. Vector $\mathcal{Z}$ has mutually independent components if and only if its joint density equals the product of its marginal densities

$$p_z(\mathbf{z}) = \prod_{i=1}^{k} p_{z_i}(z_i). \tag{3}$$

To measure the independence among the components of the random vector $\mathcal{Z}$, Comon [7] introduces an optimization criterion by calculating the Kullback–Leibler divergence (or relative entropy) of the two probability density functions corresponding to the left-hand and right-hand sides of

$$I(p_z) = \int p_z(\mathbf{z}) \log \frac{p_z(\mathbf{z})}{\prod p_{z_i}(z_i)} d\mathbf{z}. \tag{4}$$

$I(p_z)$ now defines the average mutual information of $\mathcal{Z}$. Equations (3) and (4) reveal that the mutual information vanishes if and only if the random vector $\mathcal{Z}$ has mutually independent components. Comon [7] further shows that (4) can be rewritten as follows:

$$I(p_z) = J(p_z) - \sum J(p_{z_i}) + \frac{1}{2} \log \frac{\prod V_{ii}}{|V|} \tag{5}$$

where V is the covariance matrix of $\mathcal{Z}$, and $J(p_z)$ is the negentropy, a measure of similarity between a density $p_z(\mathbf{z})$ and the Gaussian density $\phi_z(\mathbf{z})$

$$J(p_z) = -\int p_z(\mathbf{z}) \log \frac{\phi_z(\mathbf{z})}{p_z(\mathbf{z})} d\mathbf{z}. \tag{6}$$

Equations (5) and (6) provide a way to approximate the mutual information. Comon's ICA algorithm [7] applies an optimization procedure to minimize the mutual information and it consists of three major steps: 1) a singular value decomposition (SVD) procedure, which involves only low-order statistics, cancels the last term of (5); 2) a number of rotation transformations, which apply high-order statistics by means of κ-statistics, minimize the second term on the right-hand side of (5) while keeping the others unchanged; and 3) a normalization procedure, which standardizes the column vectors of W in (1) in terms of order, norm, and phase, defines a unique ICA transformation. To summarize, the algorithm that derives the ICA transformation matrix W in (1) consists of the following steps.

1) Form a data matrix using the training RGB color images

$$\mathcal{D} = \begin{bmatrix} r_1, r_2, \cdots, r_{tmn} \\ g_1, g_2, \cdots, g_{tmn} \\ b_1, b_2, \cdots, b_{tmn} \end{bmatrix}$$

where $m \times n$ and t are the spatial resolution and the number of the training images, respectively.

2) Apply Comon's ICA algorithm [7] to the data matrix $\mathcal{D}$ to derive the ICA transformation matrix W by means of three operations: an SVD procedure, a number of rotation transformations, and a normalization procedure for obtaining a unique ICA transformation.

The ICA transformation matrix $W \in \mathbb{R}^{3 \times 3}$ [see (2)], derived by Comon's algorithm [7], transforms the 3-D vector $\mathcal{X} \in \mathbb{R}^3$ in the RGB color space to a new 3-D vector $\mathcal{Z} \in \mathbb{R}^3$ with independent color components. The new color space where the 3-D vector $\mathcal{Z}$ resides is the ICA color space. Just as the RGB color space has the R, G, and B color component images, the ICA color space has three color component images as well. But contrary to the correlation property among the R, G, and B images, the three color component images in the ICA color space are independent and therefore uncorrelated. Let the three color component images in the ICA color space be $\mathbf{C}_1$, $\mathbf{C}_2$, and $\mathbf{C}_3$. As the original color image $\mathbf{C}$ has a spatial resolution of $m \times n$, the three independent color component images in the ICA color space $\mathbf{C}_1$, $\mathbf{C}_2$, and $\mathbf{C}_3$ have the same spatial resolution of $m \times n$ as well. Without loss of generality, we still use $\mathbf{C}_1$, $\mathbf{C}_2$, and $\mathbf{C}_3$ to represent the column vectors converted from the three independent color component images: $\mathbf{C}_1, \mathbf{C}_2, \mathbf{C}_3 \in \mathbb{R}^N$, where $N = mn$.

To form an effective color image representation, we first calculate the mean value and the standard deviation of the N elements inside each column vector, and let m_1, m_2, and m_3 and σ_1, σ_2, and σ_3 be the mean values and the standard deviations of $\mathbf{C}_1$, $\mathbf{C}_2$, and $\mathbf{C}_3$, respectively. We then concatenate these three column vectors (corresponding to the color component images)

to form a new pattern vector $\mathcal{Y} \in \mathbb{R}^{3N}$ by normalizing each color column vector to zero mean and unit variance

$$\mathcal{Y} = \left(\frac{\mathbf{C}_1^t - m_1}{\sigma_1} \ \ \frac{\mathbf{C}_2^t - m_2}{\sigma_2} \ \ \frac{\mathbf{C}_3^t - m_3}{\sigma_3} \right)^t \tag{7}$$

where the subtraction of a number (the mean value) from a vector is evaluated by subtracting the number from every element of the vector. The reason of normalizing each column vector to zero mean and unit variance before the concatenation is to avoid that one vector excessively dominates the others. The augmented pattern vector $\mathcal{Y}$ thus forms the new effective color image representation in the ICA color space. Next, we will discuss how to use such an effective color image representation to improve pattern recognition performance.

IV. ICA Color Space for Efficient Color Image Classification

This section discusses implementing efficient color image classification using both the effective color image representation ($\mathcal{Y}$) in the ICA color space and an enhanced Fisher model or EFM [25] for extracting the discriminating features from $\mathcal{Y}$ for classification. As $\mathcal{Y} \in \mathbb{R}^{3N}$ resides in a high-dimensional vector space, we first apply PCA to reduce the dimensionality of the vector space. Specifically, let $\Sigma_{\mathcal{Y}}$ be the covariance matrix of $\mathcal{Y}$: $\Sigma_{\mathcal{Y}} = \mathcal{E}\{[\mathcal{Y} - \mathcal{E}(\mathcal{Y})][\mathcal{Y} - \mathcal{E}(\mathcal{Y})]^t\}$, then PCA factorizes $\Sigma_{\mathcal{Y}}$ into the following form: $\Sigma_{\mathcal{Y}} = \Phi \Lambda \Phi^t$, where $\Phi = [\phi_1 \phi_2 \ldots \phi_{3N}]$ is an orthogonal eigenvector matrix and $\Lambda = \text{diag}\{\lambda_1, \lambda_2, \ldots, \lambda_{3N}\}$ a diagonal eigenvalue matrix with diagonal elements in decreasing order ($\lambda_1 \geq \lambda_2 \geq \cdots \geq \lambda_{3N}$). $\phi_1, \phi_2, \ldots, \phi_{3N}$ and $\lambda_1, \lambda_2, \ldots, \lambda_{3N}$ are the eigenvectors and the eigenvalues of $\Sigma_{\mathcal{Y}}$, respectively. The dimensionality of the pattern vector $\mathcal{Y}$ can be reduced from $3N$ to K ($K < 3N$) using the K eigenvectors corresponding to the K largest eigenvalues

$$\mathcal{U} = P^t \mathcal{Y} \tag{8}$$

where $P = [\phi_1 \phi_2 \ldots \phi_K]$. As a result, the lower dimensional pattern vector $\mathcal{U} \in \mathbb{R}^K$ captures the most expressive features of the original pattern vector $\mathcal{Y}$.

PCA, however, produces only the most expressive features that are not suitable for pattern classification. One solution to this problem is to apply the Fisher linear discriminant (FLD) analysis [11] to the lower dimensional pattern vector $\mathcal{U} \in \mathbb{R}^K$ to derive the most discriminating features for pattern recognition. Note that applying PCA for dimensionality reduction and then FLD for discriminant analysis has been suggested by many research groups [2], [8], [38]. For PCA, the more principal components are used, the better the quality of image reconstruction becomes. The same reasoning, however, does not apply to the FLD discrimination analysis. One can actually show that using more principal components can actually lead to decreased classification performance [25]. The explanation for such behavior is that the trailing eigenvalues (resulting from the more principal components used) correspond to high-frequency components and usually encode noise. When these trailing and small valued eigenvalues are included to define the reduced PCA space, FLD has to fit for noise as well and as a consequence overfitting takes

place [25]. The enhanced Fisher models address the overfitting problem and would display increased generalization performance [25]. Next we briefly review the EFM method and apply it to implement efficient color image classification.

Let $\omega_1, \omega_2, \ldots, \omega_L$ denote the classes, and $M_1, M_2, \ldots, M_L$ and M be the means of the classes and the grand mean, respectively. The within-class and between-class scatter matrices Σ_w and Σ_b are defined as follows [11]:

$$\Sigma_w = \sum_{i=1}^{L} P(\omega_i) \mathcal{E} \left\{ (\mathcal{U} - M_i)(\mathcal{U} - M_i)^t | \omega_i \right\} \tag{9}$$

$$\Sigma_b = \sum_{i=1}^{L} P(\omega_i)(M_i - M)(M_i - M)^t \tag{10}$$

where $P(\omega_i)$ is *a priori* probability. FLD derives a projection matrix Ψ by maximizing the criterion $J_1 = tr(\Sigma_w^{-1} \Sigma_b)$ [11]. This criterion is maximized when Ψ consists of the eigenvectors of the matrix $\Sigma_w^{-1} \Sigma_b$ [11]

$$\Sigma_w^{-1} \Sigma_b \Psi = \Psi \Delta \tag{11}$$

where Ψ, Δ are the eigenvector and eigenvalue matrices of $\Sigma_w^{-1} \Sigma_b$, respectively. The most discriminating features are derived by projecting the pattern vector $\mathcal{U}$ onto the eigenvectors in Ψ

$$\mathcal{V} = \Psi^t \mathcal{U}. \tag{12}$$

$\mathcal{V}$ thus contains the most discriminating features for pattern recognition.

Further study reveals that in order to improve the generalization performance of the FLD method, one should keep a proper balance between the energy criterion—the need that the selected eigenvalues (corresponding to the principal components for the original pattern vector space) account for most of the spectral energy of the raw data, for representation adequacy, and the magnitude criterion—the requirement that the eigenvalues of the within-class scatter matrix (in the reduced PCA space) are not too small, for generalization improvement [25]. In particular, the EFM method improves the generalization capability of the FLD method by decomposing the FLD procedure into a simultaneous diagonalization of the within- and between-class scatter matrices [25]. The simultaneous diagonalization is stepwise equivalent to two operations as pointed out by Fukunaga [11]: whitening the within-class scatter matrix and applying PCA to the between-class scatter matrix using the transformed data. The stepwise operation shows that during whitening the eigenvalues of the within-class scatter matrix appear in the denominator. Since the small (trailing) eigenvalues tend to capture noise [25], they cause the whitening step to fit for misleading variations, which leads to poor generalization performance. To achieve enhanced performance, the EFM method preserves a proper balance between the need that the selected eigenvalues account for most of the spectral energy of the raw data (for representational adequacy), and the requirement that the eigenvalues of the within-class scatter matrix (in the reduced PCA space) are not too small (for better generalization performance) [25].

The EFM method thus derives an appropriate low-dimensional representation [the most expressive feature vector $\mathcal{U}$ in (8)] and further extracts the discriminating features [the most discriminating feature vector $\mathcal{V}$ in (12)] from $\mathcal{U}$ for efficient color image classification. Image classification is implemented by computing the similarity score between a target discriminating feature vector and a query discriminating feature vector. Specifically, let $\mathcal{T}_i$ be a target feature vector, $i = 1, 2, \ldots, T$, and let $\mathcal{Q}_j$, $j = 1, 2, \ldots, Q$, be a query feature vector, then, the similarity score $\mathcal{S}(\mathcal{T}_i, \mathcal{Q}_j)$ based on similarity measure δ is calculated as follows:

$$\mathcal{S}(\mathcal{T}_i, \mathcal{Q}_j) = \delta(\mathcal{T}_i, \mathcal{Q}_j). \tag{13}$$

Different similarity measures usually lead to different image classification performance. The Euclidean or L_2 distance measure is among the most commonly used similarity measures in pattern recognition. Next we show that the normalized L_2 distance measure is equivalent to the cosine similarity measure for pattern recognition. Let δ_{L_2} and $\delta_{\cos}$ represent the L_2 distance measure and the cosine similarity measure, respectively. δ_{L_2} and $\delta_{\cos}$ may be formulated as follows:

$$\delta_{L_2}(\mathbf{u}, \mathbf{v}) = \left[(\mathbf{u} - \mathbf{v})^t (\mathbf{u} - \mathbf{v}) \right]^{1/2} \tag{14}$$

$$\delta_{\cos}(\mathbf{u}, \mathbf{v}) = \frac{\mathbf{u}^t \mathbf{v}}{\|\mathbf{u}\| \|\mathbf{v}\|} \tag{15}$$

where $\mathbf{u}, \mathbf{v} \in \mathbb{R}^K$ are two pattern vectors and $\| \cdot \|$ denotes the norm operator. From (14) and (15), we can derive the relationship between the L_2 distance measure and the cosine similarity measure

$$\|\mathbf{u} - \mathbf{v}\|^2 = \|\mathbf{u}\|^2 + \|\mathbf{v}\|^2 - 2\|\mathbf{u}\| \|\mathbf{v}\| \cos(\mathbf{u}, \mathbf{v}) \tag{16}$$

where $\cos(\cdot, \cdot)$ is the cosine of the angle between two vectors. If the pattern vectors $\mathbf{u}$ and $\mathbf{v}$ are normalized to have unit norm, then (16) becomes

$$[\delta_{L_2}(\mathbf{u}, \mathbf{v})]^2 = 2 - 2\delta_{\cos}(\mathbf{u}, \mathbf{v}). \tag{17}$$

Equation (17) shows that the cosine similarity measure and the normalized L_2 distance measure are equivalent for pattern recognition—a pattern recognition system that applies either the maximum cosine similarity measure or the minimum normalized L_2 distance measure (i.e., the L_2 distance measure with pattern vectors normalized to unit norm) will achieve the same classification performance. For a general discussion of the relationship among some popular similarity measures and their pattern recognition performance, see [24]. The similarity measure δ of (13) used in our experiments is the cosine similarity measure $\delta_{\cos}$.

V. EXPERIMENTS

This section assesses the effectiveness of the ICA color space method using a complex grand challenge pattern recognition problem and a large scale database, i.e., the face recognition grand challenge or FRGC problem and the FRGC version 2 database [32]. The biometric experimentation environment or BEE provides an FRGC baseline algorithm, which is a PCA al-

TABLE I
NUMBER OF IMAGES AND IMAGE QUALITY (CONTROLLED, UNCONTROLLED) OF TRAINING, TARGET, AND QUERY SETS FOR THE FRGC VERSION 2 EXPERIMENT 4

Database	Experiment	Set	Images	Image Quality
FRGC Version 2	Experiment 4	Training	12,776	Controlled or Uncontrolled
		Target	16,028	Controlled
		Query	8,014	Uncontrolled

gorithm optimized for large scale problems [3], [26], [32]. The FRGC baseline algorithm shows that the FRGC version 2 Experiment 4, which is designed for indoor controlled single still image versus uncontrolled single still image, is the most challenging FRGC experiment. We therefore choose this FRGC experiment to assess the ICA color space method. For Experiment 4, the FRGC version 2 database contains 12 776 training images, 16 028 controlled target images, and 8014 uncontrolled query images. Table I shows the number of images and image quality (controlled, uncontrolled) of the training, target, and query sets for the FRGC Experiment 4.

Face images are first cropped to extract the facial region that contains only face, so that the performance of face recognition is not affected by factors not related to face, such as background or hair styles. Fig. 2 shows some example FRGC images used in our experiments that are already cropped to the size of 64×64 to extract the facial region. In particular, the top row displays four training images: two controlled images (the first two images) and two uncontrolled images (the remaining two images). The bottom row shows a target image (the first image, which is controlled) and three query images (the remaining three images, which are uncontrolled). Note that the uncontrolled face images usually contain challenging factors, such as large illumination variations, that affect the face recognition performance.

The ICA color space is derived using Comon's ICA algorithm [7] to compute the vector $\mathcal{Z}$ [with independent components—see (2)] from the pattern vector $\mathcal{X}$ defined in the RGB color space. The number of the training vectors $\mathcal{X}$ equals the multiplication of the number of pixels ($4,096 = 64 \times 64$) in each training color image and the number of all the training images (12 776). Comon's ICA algorithm [7] applies a three-step optimization procedure (SVD, rotation transformations, and normalization) to minimize the mutual information and derive the W matrix in (2).

Given a face image in the RGB color space, the 4096 (64×64) 3-D vectors $\mathcal{X}$ can be transformed into 4096 3-D vectors $\mathcal{Z}$ using (2). These 4096 3-D vectors $\mathcal{Z}$ define three 64×64 component images, $\mathbf{C}_1$, $\mathbf{C}_2$, and $\mathbf{C}_3$, corresponding to the first, second, and third components of $\mathcal{Z}$, respectively. These $\mathbf{C}_1$, $\mathbf{C}_2$, and $\mathbf{C}_3$ images are the independent component images in the ICA color space. Fig. 3 shows some example component images in the RGB and the ICA color spaces, respectively. Specifically, the top row shows the R, G, and B component images in the RGB color space, and the bottom row displays the $\mathbf{C}_1$, $\mathbf{C}_2$, and $\mathbf{C}_3$ independent component images in the ICA color space.

Face recognition performance is evaluated using the ROC curves, which plot the FVR versus the FAR. When a similarity

Fig. 2. Example FRGC images cropped to the size of 64×64. The top row displays two controlled training images (the first two images) and two uncontrolled training images. The bottom row shows one controlled target image (the first image) and three uncontrolled query images.

Fig. 3. Example color component images in the RGB and the ICA color spaces, respectively. The top row shows the R, G, and B component images in the RGB color space, and the bottom row displays the $\mathbf{C}_1$, $\mathbf{C}_2$, and $\mathbf{C}_3$ independent component images in the ICA color space.

matrix is provided to the BEE system, it generates three ROC curves (ROC I, ROC II, and ROC III) corresponding to the images collected within semesters, within a year, and between semesters, respectively [32]. The similarity matrix stores the similarity score of every target versus query image pair. As a result, the size of the similarity matrix is $T \times Q$, i.e., the number of target images T multiplies the number of query images Q ($T = 16\,028$ and $Q = 8014$ for the FRGC version 2 Experiment 4), and the elements (similarity scores) of the similarity matrix are computed using (13).

We now assess the face recognition performance of the ICA color space method. The three independent color component images in the ICA color space $\mathbf{C}_1$, $\mathbf{C}_2$, and $\mathbf{C}_3$ are first converted into vectors. These vectors are then normalized to zero mean and unit variance, and finally concatenated to form a new pattern vector $\mathcal{Y}$ [see (7)]. The new pattern vector $\mathcal{Y}$ thus resides in a 12 288-dimensional vector space, as the spatial resolution of the three color component images is 64×64. PCA then reduces this high-dimensional vector space into a lower dimensional space,

where the EFM method further derives the discriminating features for pattern recognition. The choice of the dimensionality of the lower dimensional space considers the issue of overfitting and generalization and follows the idea of the EFM method by examining the eigenvalue spectrum [25]. The cosine similarity measure [see (15)] further applies the EFM discriminating features to compute the similarity matrix [see (13)], and finally BEE generates the three ROC curves based on the similarity matrix.

We first assess the face recognition performance in the ICA and the RGB color spaces, respectively. Fig. 4 shows the face recognition performance, the ROC curves without any score normalization (ROC I, ROC II, and ROC III), of the FRGC version 2 Experiment 4 using the concatenated pattern vector corresponding to the three independent color component images $\mathbf{C}_1$, $\mathbf{C}_2$, and $\mathbf{C}_3$ in the ICA color space, and the concatenated pattern vector corresponding to the R, G, and B component images in the RGB color space, respectively. Note that the R, G, and B component images are first converted into column vectors, then normalized to zero mean and unit variance before they are concatenated to form a new pattern vector. For both the ICA and the RGB color spaces, the dimensionality of the concatenated pattern vectors is first reduced to 1000 by PCA, after analyzing the eigenvalue spectra [25]. As the total number of subjects (i.e., classes) of the FRGC version 2 Experiment 4 training data is 222, the rank of the between-class scatter matrix is at most 221. We therefore choose 220 EFM features after the EFM analysis in the 1000 dimensional space. Equation (13) applies these 220 EFM features and the cosine similarity measure [see (15)] to produce the similarity matrix, which is finally analyzed by BEE to generate the three ROC curves. The horizontal axis of Fig. 4 represents the FAR, while the vertical axis corresponds to the FVR. As these curves are generated by the BEE system, the face recognition performance of the FRGC baseline algorithm is also included for comparison. These ROC curves show that the ICA color space achieves better FVR than the RGB color space does. In particular, the ROC III curves in Fig. 4 reveal that the new ICA color space achieves the FVR of 62.15% at the FAR of 0.1%, compared to the FVR of 52.11% of the RGB color space and 11.86% of the BEE baseline algorithm at the
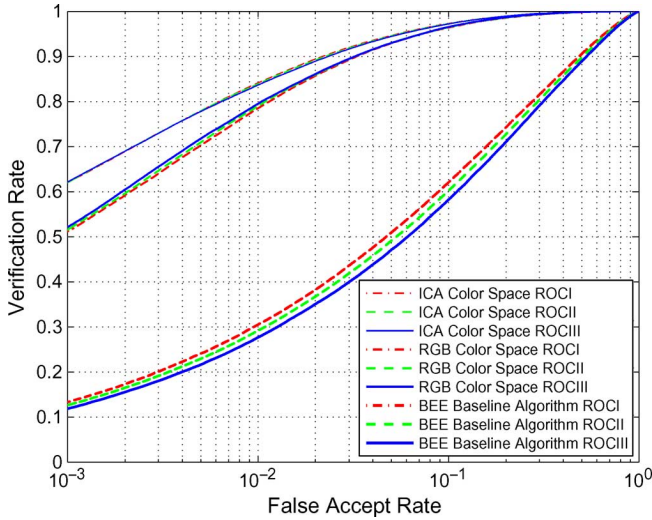
Fig. 4. Face recognition performance (without score normalization) of the FRGC version 2 Experiment 4 using the concatenated pattern vector in the ICA color space and the concatenated pattern vector in the RGB color space, respectively. The face recognition performance of the FRGC baseline algorithm is also included for comparison.
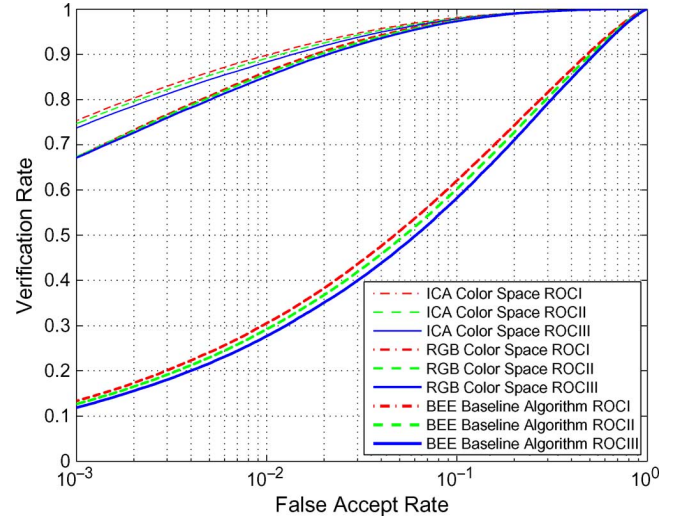

Fig. 5. Face recognition performance (with score normalization) of the FRGC version 2 Experiment 4 using the concatenated pattern vector in the ICA color space and the concatenated pattern vector in the RGB color space, respectively. The face recognition performance of the FRGC baseline algorithm is also included for comparison.

same FAR. Note that the BEE baseline algorithm applies the grayscale image that is the average of the three R, G, and B component images.

To assess the effect of score normalization on face recognition performance, we apply the z score normalization [19] on the similarity matrix. Fig. 5 shows the face recognition performance, the ROC curves with score normalization (ROC I, ROC II, and ROC III), of the FRGC version 2 Experiment 4 using the concatenated pattern vector corresponding to the three independent color component images in the ICA color space, the concatenated pattern vector corresponding to the R, G, and B component images in the RGB color space, respectively. Again, the ROC curves show that the ICA color space achieves better FVR than the RGB color space does. In particular, the ROC III curves in Fig. 5 show that the new ICA color space achieves the FVR of 73.69% at the FAR of 0.1%, compared to the FVR of 67.13% of the RGB color space at the same FAR.

Table II summarizes the ROC III FVRs at 0.1% FAR using the concatenated pattern vector in the ICA color space and the concatenated pattern vector in the RGB color space, respectively. The FRGC baseline performance is included as well for comparison. These experimental results show that the ICA color space improves upon the RGB color space for face recognition.

We then assess the comparative face recognition performance of the ICA color space method and a PCA color space method [29] in both 2-D and 3-D color spaces. To evaluate the contributions of the color transformations (ICA versus PCA) to the face recognition performance, we apply the same PCA dimensionality reduction procedure and the same EFM feature extraction procedure to the color component images derived by ICA and PCA, respectively. Fig. 6 shows the FRGC version 2 Experiment 4 face recognition performance (without score normalization), the ROC curves (ROC I, ROC II, and ROC III), of the ICA color space method and the PCA color space method in 3-D color spaces. While the ICA color space method uses the

TABLE II
FRGC VERSION 2 EXPERIMENT 4 ROC III FVRs AT 0.1% FAR USING THE CONCATENATED PATTERN VECTOR IN THE ICA COLOR SPACE AND THE CONCATENATED PATTERN VECTOR IN THE RGB COLOR SPACE, RESPECTIVELY. THE FRGC BASELINE PERFORMANCE IS INCLUDED FOR COMPARISON

Method	FVR at 0.1% FAR (ROC III)
ICA color space with score normalization	73.69%
RGB color space with score normalization	67.13%
ICA color space without score normalization	62.15%
RGB color space without score normalization	52.11%
FRGC Baseline Algorithm	11.86%

concatenated pattern vector corresponding to the three independent color component images in the ICA color space, the PCA color space method utilizes the concatenated pattern vector corresponding to the three uncorrelated component images derived by PCA. The ROC curves show that the ICA color space method achieves better FVR than the PCA color space method. In particular, the ROC III curves in Fig. 6 show that the ICA color space method achieves the FVR of 62.15% at the FAR of 0.1%, compared to the FVR of 54.95% of the PCA color space method at the same FAR. Fig. 7 shows the FRGC version 2 Experiment 4 face recognition performance (with score normalization), the ROC curves (ROC I, ROC II, and ROC III), of the ICA color space method and the PCA color space method in 3-D color spaces. Again, the ROC curves show that the ICA color space method achieves better FVR than the PCA color space method. In particular, the ROC III curves in Fig. 7 show that the ICA color space method achieves the FVR of 73.69% at the FAR of 0.1%, compared to the FVR of 69.92% of the PCA color space method at the same FAR.

We now assess the comparative face recognition performance of the ICA color space method and the PCA color space method
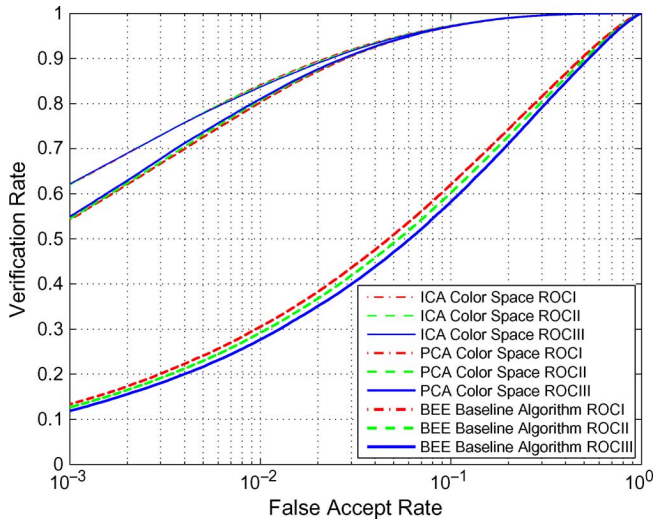
Fig. 6. FRGC version 2 Experiment 4 face recognition performance (without score normalization), the ROC curves (ROC I, ROC II, and ROC III), of the ICA color space method and the PCA color space method in 3-D color spaces. The face recognition performance of the FRGC baseline algorithm is also included for comparison.
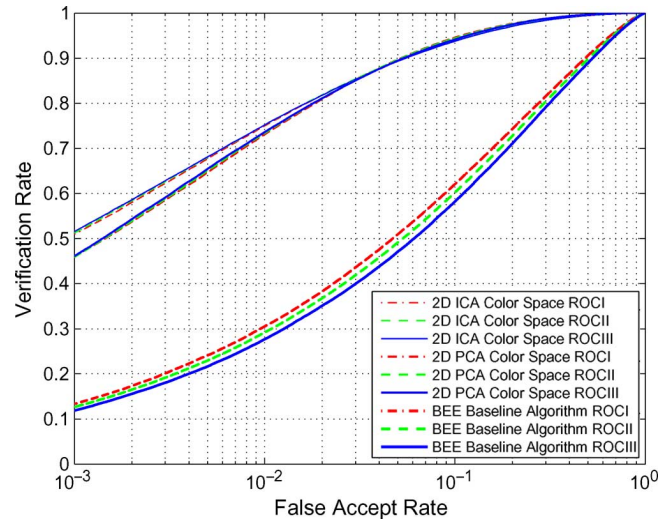

Fig. 8. FRGC version 2 Experiment 4 face recognition performance (without score normalization), the ROC curves (ROC I, ROC II, and ROC III), of the ICA color space method and the PCA color space method in 2-D color spaces. The face recognition performance of the FRGC baseline algorithm is also included for comparison.
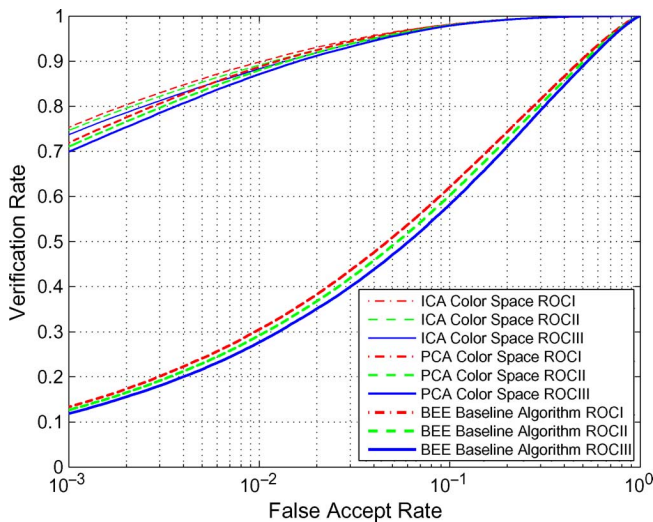

Fig. 7. FRGC version 2 Experiment 4 face recognition performance (with score normalization), the ROC curves (ROC I, ROC II, and ROC III), of the ICA color space method and the PCA color space method in 3-D color spaces. The face recognition performance of the FRGC baseline algorithm is also included for comparison.
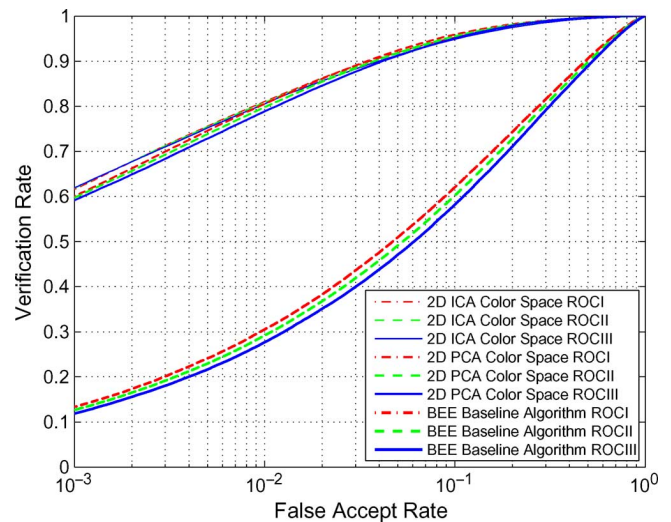

Fig. 9. FRGC version 2 Experiment 4 face recognition performance (with score normalization), the ROC curves (ROC I, ROC II, and ROC III), of the ICA color space method and the PCA color space method in 2-D color spaces. The face recognition performance of the FRGC baseline algorithm is also included for comparison.

in 2-D color spaces. Fig. 8 shows the FRGC version 2 Experiment 4 face recognition performance (without score normalization), the ROC curves (ROC I, ROC II, and ROC III), of the ICA color space method and the PCA color space method in 2-D color spaces. While the ICA color space method uses the concatenated pattern vector corresponding to the first two independent color component images in the ICA color space, the PCA color space method utilizes the concatenated pattern vector corresponding to the first two uncorrelated component images derived by PCA. The ROC curves show that the ICA color space method achieves better FVR than the PCA color space method. In particular, the ROC III curves in Fig. 8 show that the ICA color space method achieves the FVR of 51.58% at the FAR of 0.1%, compared to the FVR of 46.14% of the PCA color

space method at the same FAR. Fig. 9 shows the FRGC version 2 Experiment 4 face recognition performance (with score normalization), the ROC curves (ROC I, ROC II, and ROC III), of the ICA color space method and the PCA color space method in 2-D color spaces. Again, the ROC curves show that the ICA color space method achieves better FVR than the PCA color space method. In particular, the ROC III curves in Fig. 9 show that the ICA color space method achieves the FVR of 61.93% at the FAR of 0.1%, compared to the FVR of 59.16% of the PCA color space method at the same FAR.

Table III summarizes the ROC III FVRs at 0.1% FAR of the ICA color space method and the PCA color space method in 2-D and 3-D color spaces. The FRGC baseline performance is included as well for comparison. The experimental results in

TABLE III
FRGC VERSION 2 EXPERIMENT 4 ROC III FVRS AT 0.1% FAR OF THE ICA
COLOR SPACE METHOD AND THE PCA COLOR SPACE METHOD IN 2-D
AND 3-D COLOR SPACES. THE FRGC BASELINE PERFORMANCE
IS INCLUDED FOR COMPARISON

Method	FVR at 0.1% FAR (ROC III)
ICA color space method in 3D color space with score normalization	73.69%
PCA color space method in 3D color space with score normalization	69.92%
ICA color space method in 3D color space without score normalization	62.15%
PCA color space method in 3D color space without score normalization	54.95%
ICA color space method in 2D color space with score normalization	61.93%
PCA color space method in 2D color space with score normalization	59.16%
ICA color space method in 2D color space without score normalization	51.58%
PCA color space method in 2D color space without score normalization	46.14%
FRGC Baseline Algorithm	11.86%

2-D color spaces are much worse than those in 3-D color spaces for both the ICA color space method and the PCA color space method. The experimental results also reveal that the ICA color space method improves upon the PCA color space method for face recognition.

VI. CONCLUSION

This paper presents an ICA color space method for pattern recognition. The ICA color space, derived by means of ICA of the RGB color space, defines three new component images that are more effective than the tristimuli R, G, and B component images for pattern recognition. In contrast to the RGB color space, where the R, G, and B component images are correlated, the new ICA color space defines three component images that are independent and hence uncorrelated. As the ICA algorithm performs the blind source separation, the three component images in the ICA color space are formed by the independent color sources, and should encode more discriminating power than the R, G, and B component images for classification. Experiments using a complex grand challenge pattern recognition problem together with a large scale database show that the proposed ICA color space is more effective than the RGB color space for face recognition.

ACKNOWLEDGMENT

REFERENCES

[1] M. S. Bartlett, J. R. Movellan, and T. J. Sejnowski, "Face recognition by independent component analysis," *IEEE Trans. Neural Netw.*, vol. 13, no. 6, pp. 1450–1464, Nov. 2002.

[2] P. N. Belhumeur, J. P. Hespanha, and D. J. Kriegman, "Eigenfaces vs. Fisherfaces: Recognition using class specific linear projection," *IEEE Trans. Pattern Anal. Mach. Intell.*, vol. 19, no. 7, pp. 711–720, Jul. 1997.

[3] J. R. Beveridge, D. Bolme, B. A. Draper, and M. Teixeira, "The csu face identification evaluation system: Its purpose, features, and structure," *Mach. Vis. Appl.*, vol. 16, no. 2, pp. 128–138, 2005.
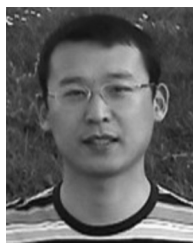
[4] K. W. Bowyer, K. Chang, and P. J. Flynn, "A survey of approaches and challenges in 3D and multi-modal 3D+2D face recognition," *Comput. Vis. Image Understand.*, vol. 101, no. 1, pp. 1–15, 2006.

[5] K. W. Bowyer, K. I. Chang, P. Yan, P. J. Flynn, E. Hansley, and S. Sarkar, "Multi-modal biometrics: An overview," in *Proc. 2nd Workshop MultiModal User Authentication*, Toulouse, France, 2006 [Online]. Available: http://mmua.cs.ucsb.edu/MMUA2006/Papers/Bowyer_MMUA.pdf

[6] R. Cappelli, D. Maio, D. Maltoni, J. L. Wayman, and A. K. Jain, "Performance evaluation of fingerprint verification systems," *IEEE Trans. Pattern Anal. Mach. Intell.*, vol. 28, no. 7, pp. 3–18, Jul. 2006.

[7] P. Comon, "Independent component analysis, a new concept?," *Signal Process.*, vol. 36, pp. 287–314, 1994.

[8] K. Etemad and R. Chellappa, "Discriminant analysis for recognition of human face images," *J. Opt. Soc. Amer. A*, vol. 14, pp. 1724–1733, 1997.

[9] G. D. Finlayson, S. S. Chatterjee, and B. V. Funt, "Color angular indexing," in *Proc. Eur. Conf. Comput. Vis.*, Cambridge, U.K., Apr. 14–18, 1996, pp. 16–27.

[10] G. D. Finlayson, S. D. Hordley, and P. M. Hubel, "Color by correlation: A simple, unifying framework for color constancy," *IEEE Trans. Pattern Anal. Mach. Intell.*, vol. 23, no. 11, pp. 1209–1221, Nov. 2001.

[11] K. Fukunaga, *Introduction to Statistical Pattern Recognition*, 2nd ed. New York: Academic, 1990.

[12] C. Garcia and G. Tziritas, "Face detection using quantized skin color regions merging and wavelet packet analysis," *IEEE Trans. Multimedia*, vol. 1, no. 3, pp. 264–277, Sep. 1999.

[13] J. M. Geusebroek, R. van den Boomgaard, A. W. M. Smeulders, and H. Geerts, "Color invariance," *IEEE Trans. Pattern Anal. Mach. Intell.*, vol. 23, no. 12, pp. 1338–1350, Dec. 2001.

[14] R. C. Gonzalez and R. E. Woods, *Digital Image Processing*, 2nd ed. Englewood Cliffs, NJ: Prentice-Hall, 2002.

[15] G. Healey and D. A. Slater, "Global color constancy: Recognition of objects by use of illumination invariant properties of color distributions," *J. Opt. Soc. Amer. A*, vol. 11, no. 11, pp. 3003–3010, 1994.

[16] K. E. Hild, H. T. Attias, and S. S. Nagarajan, "An expectation-maximization method for spatio-temporal blind source separation using an ar-mog source model," *IEEE Trans. Neural Netw.*, vol. 19, no. 3, pp. 508–519, Mar. 2008.

[17] E. Hjelmas and B. K. Low, "Face detection: A survey," *Comput. Vis. Image Understand.*, vol. 83, pp. 236–274, 2001.

[18] R. L. Hsu, M. Abdel-Mottaleb, and A. K. Jain, "Face detection in color images," *IEEE Trans. Pattern Anal. Mach. Intell.*, vol. 24, no. 5, pp. 696–706, May 2002.

[19] A. K. Jain, K. Nandakumar, and A. Ross, "Score normalization in multimodel biometric systems," *Pattern Recognit.*, vol. 38, pp. 2270–2285, 2005.

[20] A. K. Jain, S. Pankanti, S. Prabhakar, L. Hong, and A. Ross, "Biometrics: A grand challenge," in *Proc. 17th Int. Conf. Pattern Recognit.*, 2004, pp. 935–942.

[21] C. F. Jones, III and A. L. Abbott, "Optimization of color conversion for face recognition," *EURASIP J. Appl. Signal Process.*, vol. 2004, no. 4, pp. 522–529, 2004.

[22] J. Karhunen, E. Oja, L. Wang, R. Vigario, and J. Joutsensalo, "A class of neural networks for independent component analysis," *IEEE Trans. Neural Netw.*, vol. 8, no. 3, pp. 486–504, May 1997.

[23] C. Liu, "Capitalize on dimensionality increasing techniques for improving face recognition grand challenge performance," *IEEE Trans. Pattern Anal. Mach. Intell.*, vol. 28, no. 5, pp. 725–737, May 2006.

[24] C. Liu, "The Bayes decision rule induced similarity measures," *IEEE Trans. Pattern Anal. Mach. Intell.*, vol. 29, no. 6, pp. 1086–1090, Jun. 2007.

[25] C. Liu and H. Wechsler, "Robust coding schemes for indexing and retrieval from large face databases," *IEEE Trans. Image Process.*, vol. 9, no. 1, pp. 132–137, Jan. 2000.

[26] H. Moon and P. J. Phillips, "Computational and performance aspects of PCA-based face-recognition algorithms," *Perception*, vol. 30, pp. 303–321, 2001.

[27] V. E. Neagoe, "Color space projection, feature fusion and concurrent neural modules for biometric image recognition," in *Proc. 5th WSEAS Int. Conf. Comput. Intell., Man-Mach. Syst. Cybern.*, Venice, Italy, Nov. 20–22, 2006, pp. 286–291.

[28] V. E. Neagoe, "An optimum color feature space and its applications for pattern recognition," *WSEAS Trans. Signal Process.*, vol. 2, no. 12, pp. 1537–1543, 2006.

[29] V. E. Neagoe, "An optimum 2D color space for pattern recognition," in *Proc. Int. Conf. Image Process. Comput. Vis. Pattern Recognit.*, Las Vegas, NV, Jun. 26–29, 2006, pp. 526–532.

[30] B. A. Olshausen and D. J. Field, "Emergence of simple-cell receptive field properties by learning a sparse code for natural images," *Nature*, vol. 381, no. 13, pp. 607–609, 1996.

[31] S. Pankanti, R. M. Bolle, and A. Jain, "Guest editors' introduction: Biometrics-the future of identification," *Computer*, vol. 33, no. 2, pp. 46–49, 2000.

[32] P. J. Phillips, P. J. Flynn, T. Scruggs, K. W. Bowyer, J. Chang, K. Hoffman, J. Marques, J. Min, and W. Worek, "Overview of the face recognition grand challenge," in *Proc. IEEE Conf. Comput. Vis. Pattern Recognit.*, 2005, pp. 947–954.

[33] H. Shen, M. Kleinsteuber, and K. Huper, "Local convergence analysis of fastICA and related algorithms," *IEEE Trans. Neural Netw.*, vol. 19, no. 6, pp. 1022–1032, Jun. 2008.

[34] P. Shih and C. Liu, "Comparative assessment of content-based face image retrieval in different color spaces," *Int. J. Pattern Recognit. Artif. Intell.*, vol. 19, no. 7, pp. 873–893, 2005.

[35] A. W. M. Smeulders, M. Worring, S. Santini, A. Gupta, and R. Jain, "Content-based image retrieval at the end of the early years," *IEEE Trans. Pattern Anal. Mach. Intell.*, vol. 22, no. 12, pp. 1349–1380, Dec. 2000.

[36] K. Sobottka and I. Pitas, "Segmentation and tracking of faces in color images," in *Proc. 2nd Int. Conf. Autom. Face Gesture Recognit.*, Killington, VT, Oct. 13–16, 1996, pp. 236–241.

[37] M. J. Swain and D. H. Ballard, "Color indexing," *Int. J. Comput. Vis.*, vol. 7, no. 1, pp. 11–32, 1991.

[38] D. L. Swets and J. Weng, "Using discriminant eigenfeatures for image retrieval," *IEEE Trans. Pattern Anal. Mach. Intell.*, vol. 18, no. 8, pp. 831–836, Aug. 1996.

[39] T. T. Tan and K. Ikeuchi, "Separating reflection components of textured surfaces using a single image," *IEEE Trans. Pattern Anal. Mach. Intell.*, vol. 27, no. 2, pp. 178–193, Feb. 2001.

[40] J. C. Terrillon, M. N. Shirazi, H. Fukamachi, and S. Akamatsu, "Comparative performance of different skin chrominance models and chrominance space for the automatic detection of human faces in color images," in *Proc. 4th Int. Conf. Face Gesture Recognit.*, Grenoble, France, Mar. 28–30, 2000, pp. 54–61.

[41] P. Tichavsky, Z. Koldovsky, A. Yeredor, G. Gomez-Herrero, and E. Doron, "A hybrid technique for blind separation of non-Gaussian and time-correlated sources using a multicomponent approach," *IEEE Trans. Neural Netw.*, vol. 19, no. 3, pp. 421–430, Mar. 2008.

[42] W. Zhao, R. Chellappa, J. Phillips, and A. Rosenfeld, "Face recognition: A literature survey," *ACM Comput. Surv.*, vol. 35, no. 4, pp. 399–458, 2003.

Chengjun Liu received the Ph.D. degree from the Computer Science Department, George Mason University, Arlington, VA, in 1999,

Currently, he is an Associate Professor of Computer Science and the Director of the Face Recognition and Video Processing Lab, New Jersey Institute of Technology, Newark. His research interests are in pattern recognition (face/iris recognition), machine learning (statistical learning, kernel methods, similarity measures), computer vision (object/face detection, video processing), security (biometrics), and image processing (new color spaces, Gabor image representation). His recent research has been concerned with the development of novel and robust methods for image/video retrieval and object detection, tracking and recognition based upon statistical and machine learning concepts. The class of new methods he has developed includes the Bayesian discriminating features method (BDF), the probabilistic reasoning models (PRMs), the enhanced Fisher models (EFMs), the enhanced independent component analysis (EICA), the shape and texture-based Fisher method (STF), the Gabor–Fisher classifier (GFC), and the independent Gabor features (IGF) method. He has also pursued the development of novel evolutionary methods leading to the development of the evolutionary pursuit (EP) method for pattern recognition in general, and face recognition in particular.

Jian Yang received the B.S. degree in mathematics from the Xuzhou Normal University, Xuzhou, China, in 1995, the M.S. degree in applied mathematics from the Changsha Railway University, Changsha, China, in 1998, and the Ph.D. degree from the Nanjing University of Science and Technology (NUST), Nanjing, China, on the subject of pattern recognition and intelligence systems in 2002.

In 2003, he was a Postdoctoral Researcher at the University of Zaragoza, and in the same year, he was awarded the RyC program Research Fellowship sponsored by the Spanish Ministry of Science and Technology. From 2004 to 2006, he was a Postdoctoral Fellow at Biometrics Center of Hong Kong Polytechnic University. From 2006 to 2007, he was a Postdoctoral Fellow at the Department of Computer Science, New Jersey Institute of Technology. Currently, he is a Professor in the School of Computer Science and Technology, NUST. He is the author of more than 50 scientific papers in pattern recognition and computer vision. His current research interests include pattern recognition, computer vision, and machine learning.